

On-Device Interpretable Tsetlin Machine-Based Intrusion Detection for Secure IoMT

Rahul Jaiswal, Per-Arne Andersen, Linga Reddy Cenkeramaddi, Lei Jiao, Ole-Christoffer Granmo
The Centre for Artificial Intelligence Research (CAIR)
Department of ICT, University of Agder, Norway
{rahul.jaiswal, per.andersen, linga.cenkeramaddi, lei.jiao, ole.granmo}@uia.no

Abstract—The rapid evolution of digital health technologies is redefining healthcare services worldwide. The integration of wireless communication and Internet-enabled medical devices within Internet of Medical Things (IoMT) networks enables continuous, real-time patient monitoring. However, this increased connectivity raises cybersecurity and patient safety risks due to increasingly sophisticated cyberattacks. This paper proposes a novel on-device, interpretable Tsetlin Machine (TM)-based Intrusion Detection System (IDS) to identify various phases of cyberattacks in IoMT environments. The TM is a rule-driven and transparent machine learning (ML) approach that represents attack patterns using propositional logic. Extensive evaluations on the MedSec-25 dataset, encompassing various phases of realistic cyberattacks, show that the proposed model outperforms ML models and state-of-the-art methods, attaining a classification performance of 97.83%. Moreover, the proposed model offers explicit explanations of its decisions to enhance transparency using feature-level contributions, class-wise vote scores, and clause activation heatmaps. Edge deployment (Raspberry Pi) further supports real-time on-device inference and intrusion detection. The combination of interpretability and high performance makes the proposed model well-suited for IoMT healthcare, where trust, reliability, safety, and timely decision-making are critical.

Index Terms—Cybersecurity, Intrusion Detection, Internet of Medical Things, Raspberry Pi, and Tsetlin Machine.

I. INTRODUCTION

The digital health technologies are advancing rapidly, enabling easier access to online doctor consultations through better internet connectivity, smartphones, and mobile applications. This approach is not only faster and more affordable for busy professionals but also highly convenient for elderly people, especially those living in rural or remote areas. It eliminates the need for unnecessary travel to the hospital, reduces waiting time, and offers a cost-effective alternative to traditional in-person doctor visits.

In digital healthcare services, patients' health data is transmitted electronically to the healthcare providers, such as hospitals and doctors, via digital channels using wearable medical devices (e.g., smart watches), as shown in Fig. 1. The interconnected framework that enables medical devices, healthcare platforms, and digital systems to exchange medical data over the Internet is known as the Internet of Medical Things (IoMT) [1]. It enables efficient transmission of health data from patient devices to healthcare providers, improving both the timeliness and effectiveness of ongoing patient care.



Fig. 1: Overview of IoMT in healthcare.

The Deloitte Health Care Report 2026 [2] highlights that IoMT and digital health technologies are driving healthcare toward a “Care Anywhere” model, making virtual healthcare services more accessible and efficient. However, the use of IoMT medical devices introduces several critical challenges. Since these devices are connected to the Internet and continuously transmit highly sensitive medical data, they become attractive targets for cyberattacks. This raises major concerns such as unauthorized data access, medical device hijacking, exposure of sensitive personal health information, and cyberattacks that may disrupt system functionality or render medical devices unavailable, ultimately posing risks to both patient safety and privacy. For instance, if the cyberattackers alter the medical data of the patient within the hospital systems, then doctors may rely on the inaccurate readings, resulting in inappropriate treatment and potentially life-threatening harm to the patients. The CrowdStrike Global Threat Report 2026 [3] highlights that 10% of global cyberattacks target healthcare systems.

To ensure safe, secure, and reliable healthcare services, Intrusion Detection Systems (IDS) [4] are used in the IoMT networks. They utilize network-based security techniques to monitor network traffic and identify potential cyberattacks in real time. Upon detecting suspicious activities, IDS promptly alerts the network administrators about potential intrusions or cyberattacks, enabling a timely response and mitigation.

This paper presents a novel IDS system for detecting different phases of cyberattacks targeting IoMT environments by leveraging an interpretable machine learning (ML) approach based on the Tsetlin Machine (TM) [5], [6]. Building on this, network-level features are extracted from IoMT traffic and used as input to the TM model, which classifies the traffic

as benign (normal) or malicious attacks. To promote transparency and build trust in the outcome of the TM model beyond black-box ML models, the interpretability of the TM model is explicitly analyzed. Moreover, the proposed TM-based IDS is deployed on the resource-constrained edge device (Raspberry Pi) to enable on-device inference for real-time attack/intrusion detection.

The rest of this paper is structured as follows. Section II reviews the related work and outlines the motivation. Section III describes the classifiers employed and the on-device inference approach used in this study. Section IV describes the proposed TM-based intrusion detection system. Section V introduces the experimental dataset. Section VI presents and discusses the results. Finally, Section VII concludes the paper and highlights directions for future research.

II. RELATED WORK AND MOTIVATION

Intrusion Detection Systems (IDS) play a critical role in safeguarding sensitive medical data from cyberattacks within IoMT environments. It can detect both internal and external attacks that bypass existing security measures. Traditional IDS systems are broadly categorized into two approaches, namely, signature-based and anomaly-based detection [7], [8]. The signature-based approach identifies known attacks by matching observed patterns against predefined signatures. In contrast, anomaly-based detection focuses on identifying deviations from the normal network behavior to detect potential attacks. However, the highly dynamic nature of IoMT environments constrains the effectiveness of both approaches in identifying new and unseen cyberattacks, leaving IoMT devices exposed to emerging cyberattacks.

Machine learning (ML) and deep learning (DL) based intrusion detection systems have demonstrated strong potential for enhancing IoMT security. These techniques can identify attacks by detecting deviations in the attributes of network traffic. For instance, the work in [9] investigates various ML approaches for cyberattack detection on the IEEE DataPort dataset and attains an accuracy of 89.89% for binary classification using K-nearest Neighbours (KNN). In [10], a deep autoencoder-based IDS is developed to secure IoMT using the NF-ToN-IoT dataset, achieving an accuracy of 89% for 10-class classification. In [11], the authors propose deep neural network (DNN) and long short-term memory (LSTM) based models for cyberattack detection in IoMT environments using the CICIOMT24 dataset, achieving accuracies of 78% and 79%, respectively, for six-class classification. In [12], the authors apply various ML techniques for cyberattack detection, achieving an accuracy of 73.5% in a six-class classification setting. Although these ML/DL models can attain high classification accuracy, interpretability remains a critical requirement for their effective adoption in healthcare services. Moreover, many of these models operate as black boxes, providing limited insight into their decision-making processes, which raises significant concerns regarding the transparency of outcomes. The Tsetlin Machine (TM) [5], [6] has emerged as a promising alternative to address these limitations.

The TM is an emerging machine learning technique based on Tsetlin Automata [6], well-suited for IoMT intrusion detection. It focuses on identifying recurring patterns in network traffic through frequent pattern learning and efficient resource allocation, rather than relying solely on error minimization. By representing knowledge as interpretable conjunctive clauses, the TM reduces overfitting and simplifies intrusion detection into manageable patterns, making it suitable for reliable on-device intrusion detection. For instance, the study in [13] introduces a TM-based anomaly detection framework and evaluates it across multiple datasets to demonstrate improved accuracy than ML classifiers. TM is integrated with transfer learning [14], [15] to classify cervical cancer using the pap smear image dataset in [16]. A TM-based IDS using the CICIOMT24 dataset is developed in [17], achieving superior accuracy than ML/DL classifiers. These findings motivate us to propose a novel, transparent, and interpretable TM-based IDS to detect various phases of cyberattacks in IoMT environments and improve patient safety. Moreover, to demonstrate the effectiveness of the proposed IDS in real-time inference, it is also evaluated on a resource-constrained edge device, specifically a Raspberry Pi. This paper makes the following contributions:

- Development of an effective TM-based IDS to detect various phases of cyberattacks in IoMT environments.
- Evaluation of the proposed IDS in a multi-class attack detection setting using the MedSec-25 dataset.
- Numerical evidence demonstrating the superiority of the proposed IDS over state-of-the-art ML methods.
- Interpretability analysis of the proposed IDS to reveal decision rules for accurate attack detection.
- Edge deployment of the proposed IDS for real-time on-device inference and attack detection.
- Demonstration of the practical applicability of the TM-based solutions for IoMT security.

III. BACKGROUND

In this section, Tsetlin Machines, classification models, and an on-device inference approach are introduced.

A. Tsetlin Machine

The TM is an interpretable, rule-based machine learning model that constructs logical clauses using propositional logic [6]. It represents cyberattack patterns as human-readable logical expressions, thereby enabling transparent and explainable intrusion detection. Owing to its binary feature representation, TM is particularly suitable for deployment on resource-constrained devices. Additionally, TM shows strong robustness to class imbalance, a prevalent feature of IoMT datasets such as MedSec-25 (see Table II).

The TM comprises a set of conjunctive clauses defined over binary input features. A clause C_j is expressed as [6]:

$$C_j = \bigwedge_{k \in I_j} x_k \wedge \bigwedge_{l \in \bar{I}_j} \neg x_l \quad (1)$$

where $x_k \in \{0, 1\}$ denotes binary features, and I_j and \bar{I}_j represent the sets of included and negated literals, respectively.

Each clause casts a vote for or against a class, and the final prediction is obtained by aggregating clause outputs as:

$$f(\mathbf{x}) = \sum_{j=1}^m w_j C_j(\mathbf{x}), \quad \text{with } |f(\mathbf{x})| \leq T \quad (2)$$

where $w_j \in \{+1, -1\}$ denotes the polarity of clause j , and T is the voting threshold that constrains the total clause contribution, ensuring balanced learning. The clause granularity is controlled by the specificity parameter $s > 1$, which regulates the inclusion probability of literals.

Sparse Tsetlin Machine (STM): It is a variant of the TM in which, unlike the standard TM that considers all literals (both features and their negations) when forming clauses, only a subset of literals is used per clause. The STM introduces controlled sparsity, leading to fewer active features, reduced influence of irrelevant features, and improved generalization. A clause C_j in STM is expressed as [6]:

$$C_j = \bigwedge_{k \in S_j^+} x_k \wedge \bigwedge_{l \in S_j^-} \neg x_l \quad (3)$$

where $S_j^+ \subseteq 1, \dots, n$ and $S_j^- \subseteq 1, \dots, n$ denote the subsets of selected features included as positive and negated literals in clause j , respectively, with $|S_j^+ \cup S_j^-| \ll n$. n denotes the number of input features.

In multi-class classification, each class is represented by a dedicated set of clauses, which are evenly divided into positive and negative polarity groups. These clauses are formed using combinations of input features and their negations to capture class-specific patterns. For a given input, each clause evaluates to either true or false, and contributes a vote toward or against its associated class. The overall score for each class is obtained by aggregating the votes from its positive and negative clauses. Finally, the predicted label is determined by selecting the class with the highest aggregated score. The detailed mathematical formulation of TM can be seen in [17].

B. Classification Models

A brief description of the classifiers used in the experiments is presented in this section.

1) *Decision Tree (DT)*: DT is a hierarchical model composed of internal decision nodes and terminal leaf nodes. Each decision node splits the data based on a feature condition, creating multiple branches corresponding to possible outcomes. The leaf nodes represent the final class labels. The DT follows a recursive partitioning strategy, often described as a divide-and-conquer approach [18], [19].

2) *Random Forest (RF)*: RF is an ensemble learning method that constructs a collection of decision trees during training. Each tree independently predicts the class label, and the final output is determined through a majority voting mechanism across all trees [19], [20].

3) *XGBoost*: XGBoost is an advanced implementation of gradient boosting that builds an ensemble of decision trees in a sequential manner. Each subsequent tree focuses on correcting the errors made by previous ones, leading to improved predictive performance [21].

4) *LightGBM (LGBM)*: LightGBM is a gradient boosting framework which employs a leaf-wise tree growth strategy along with histogram-based feature binning to enable faster training and reduced computational cost [22].

5) *K-Nearest Neighbours (KNN)*: KNN is a distance-based classification method that assigns a class label to a test instance based on the majority class among its nearest neighbours, typically measured using Euclidean distance [20].

6) *Naive Bayes (NB)*: NB is a probabilistic classifier based on Bayes' theorem. It assumes conditional independence among input features and simplifies the classification problem by treating each feature independently [19], [23].

7) *Logistic Regression (LR)*: LR is a linear classification model that estimates class probabilities using a logistic (sigmoid) function, mapping input features between 0 and 1 [19].

8) *Neural Network (NN)*: A NN consists of multiple layers of interconnected neurons that transform input data through non-linear operations. It enables the model to learn complex patterns and relationships within the data, making it suitable for detecting sophisticated cyberattack behaviors [19].

C. On-Device Inference

To evaluate on-device inference of the TM model on a resource-constrained platform, Raspberry Pi 5 Model B [24] is employed. It is a compact and efficient computing platform, approximately the size of a credit/debit card, and serves as a powerful mini-computer (see Fig. 2). It has a quad-core ARM Cortex-A76 processor operating at 2.4 GHz and supports up to 8 GB of SDRAM. The board includes two USB 3.0 and two USB 2.0 ports, and supports Ethernet, Wi-Fi, and Bluetooth connectivity at 2.4 GHz and 5 GHz. Additionally, it supports camera, audio, and video interfaces. Its on-device deployment capability facilitates efficient execution of the TM model in the resource-constrained IoMT environments.

The Raspberry Pi is connected to the host computer via Ethernet, enabling reliable network communication between the devices. The TM and other ML models are implemented and executed in Python on the Raspberry Pi, enabling on-device inference, while development and data transfer are managed from the host system. This configuration supports seamless deployment and real-time on-device inference on the edge device (Raspberry Pi).

IV. PROPOSED INTRUSION DETECTION SYSTEM

The objective of the proposed IDS is to accurately identify and classify various phases of cyberattacks in IoMT environments. The overall architecture of the proposed TM-based IDS is illustrated in Fig. 2, comprising three main stages, namely, data preparation, model training, and edge deployment.

In the first stage, data preparation is carried out to construct a suitable input for training the TM model. This stage involves selecting the IoMT dataset, followed by preprocessing steps such as handling missing and duplicate entries, normalizing the data, and addressing class imbalance. Subsequently, feature binarization is performed to transform the input data into a binary format compatible with the TM model.

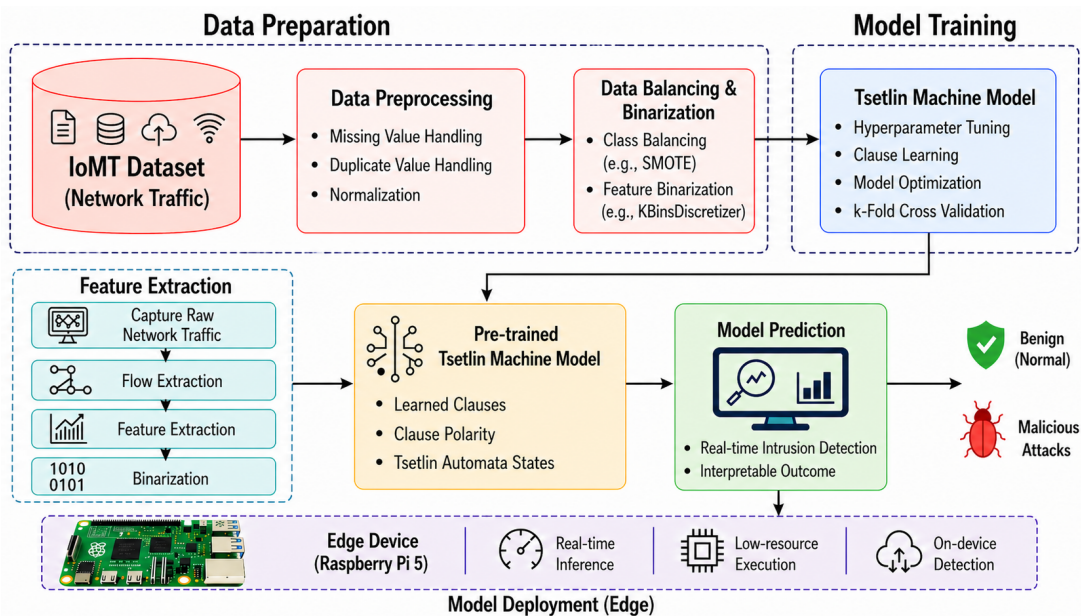


Fig. 2: Proposed TM-Based IDS architecture.

In the second stage, the TM model is trained to learn discriminative patterns from the processed data. This includes hyperparameter tuning, clause formation, and model optimization. To ensure reliable performance and reduce overfitting, k-fold cross-validation [25] is employed. During training, the TM captures interpretable logical relationships in the form of positive and negative clauses to compute class-specific scores for classification. The trained model, along with its learned clauses and automata states, is then stored for deployment.

In the final stage, the trained model is deployed on an edge device using the Raspberry Pi to enable real-time on-device inference. The network traffic is continuously captured and converted into flow-based features, which are then preprocessed and binarized before being fed into the pre-trained TM model. The model performs on-device classification to label the network traffic as *benign* or *malicious attacks*. This on-device, edge-based implementation enables low-latency detection and reduces reliance on centralized systems. Furthermore, the prediction results can be integrated with the security mechanisms, such as firewalls, to automatically block malicious activities, thereby enhancing the overall security of the IoMT networks.

V. EXPERIMENTAL DATASET

To enhance IoMT security, the MedSec-25 dataset¹ [26] presents the behavior of benign and malicious traffic within a realistic healthcare IoT network environment that reflects real-world hospital operations. The setup utilizes Raspberry Pi nodes along with various medical and environmental sensors, including Electrocardiogram (ECG), Electroencephalogram (EEG), respiration, thermistor, ultrasonic modules, and

environmental sensors. It employs a variety of IoMT devices and protocols, including Message Queuing Telemetry Transport (MQTT), Secure Shell (SSH), File Transfer Protocol (FTP), Hypertext Transfer Protocol (HTTP), and Domain Name System (DNS). The benign traffic is generated using multiple services and operations, such as HTTP-based services and real user interactions with medical devices. A multi-stage attack campaign is conducted to simulate malicious traffic, which facilitates early detection of attacks at each phase and limits further escalation. Based on the MITRE ATT&CK framework [27], the attack campaign comprises four phases, namely, reconnaissance, initial access, lateral movement, and exfiltration, capturing the major phases of real-world attacks. The generated network traffic is captured using Wireshark and stored in PCAPNG format. The flow-based network features are extracted using CICFlowMeter, and CSV files are generated for each attack phase.

Reconnaissance is the initial phase of cyberattacks, in which an adversary/cyberattacker gathers information about the target network, including active hosts, open ports, and system characteristics, using techniques such as SYN/TCP scanning and operating system (OS) fingerprinting. During the initial access phase, the adversary gains unauthorized entry into a target system or network by exploiting vulnerabilities, weak credentials, or exposed services (e.g., SSH, FTP, or web applications). After gaining initial access, the lateral movement phase enables the adversary to propagate across the network and compromise additional systems by leveraging credentials, remote services, or network weaknesses. Finally, in the exfiltration phase, the cyberattacker extracts sensitive data from compromised systems and sends it to an external destination using covert communication channels. The dataset is imbalanced, comprising 84 features and 554,534 samples, as presented in Table I and Table II, respectively.

¹Link to dataset: <https://www.kaggle.com/datasets/abdullah001234/medsec-25-iomt-cybersecurity-dataset>.

TABLE I: Feature set of the MedSec-25 dataset.

S.No.	Feature name	S.No.	Feature name	S.No.	Feature name	S.No.	Feature name	S.No.	Feature name
1.	Flow ID	2.	Src IP	3.	Src Port	4.	Dst IP	5.	Dst Port
6.	Protocol	7.	Timestamp	8.	Flow Duration	9.	Tot Fwd Pkts	10.	Tot Bwd Pkts
11.	TotLen Fwd Pkts	12.	TotLen Bwd Pkts	13.	Fwd Pkt Len Max	14.	Fwd Pkt Len Min	15.	Fwd Pkt Len Mean
16.	Fwd Pkt Len Std	17.	Bwd Pkt Len Max	18.	Bwd Pkt Len Min	19.	Bwd Pkt Len Mean	20.	Bwd Pkt Len Std
21.	Flow Byts/s	22.	Flow Pkts/s	23.	Flow IAT Mean	24.	Flow IAT Std	25.	Flow IAT Max
26.	Flow IAT Min	27.	Fwd IAT Tot	28.	Fwd IAT Mean	29.	Fwd IAT Std	30.	Fwd IAT Max
31.	Fwd IAT Min	32.	Bwd IAT Tot	33.	Bwd IAT Mean	34.	Bwd IAT Std	35.	Bwd IAT Max
36.	Bwd IAT Min	37.	Fwd PSH Flags	38.	Bwd PSH Flags	39.	Fwd URG Flags	40.	Bwd URG Flags
41.	Fwd Header Len	42.	Bwd Header Len	43.	Fwd Pkts/s	44.	Bwd Pkts/s	45.	Pkt Len Min
46.	Pkt Len Max	47.	Pkt Len Mean	48.	Pkt Len Std	49.	Pkt Len Var	50.	FIN Flag Cnt
51.	SYN Flag Cnt	52.	RST Flag Cnt	53.	PSH Flag Cnt	54.	ACK Flag Cnt	55.	URG Flag Cnt
56.	CWE Flag Count	57.	ECE Flag Cnt	58.	Down/Up Ratio	59.	Pkt Size Avg	60.	Fwd Seg Size Avg
61.	Bwd Seg Size Avg	62.	Fwd Byts/b Avg	63.	Fwd Pkts/b Avg	64.	Fwd Blk Rate Avg	65.	Bwd Byts/b Avg
66.	Bwd Pkts/b Avg	67.	Bwd Blk Rate Avg	68.	Subflow Fwd Pkts	69.	Subflow Fwd Byts	70.	Subflow Bwd Pkts
71.	Subflow Bwd Byts	72.	Init Fwd Win Byts	73.	Init Bwd Win Byts	74.	Fwd Act Data Pkts	75.	Fwd Seg Size Min
76.	Active Mean	77.	Active Std	78.	Active Max	79.	Active Min	80.	Idle Mean
81.	Idle Std	82.	Idle Max	83.	Idle Min	84.	Label	Total features = 84	

TABLE II: Attack phases in the MedSec-25 dataset.

Label	Attack phases	Sample count
0	Benign	12,348
1	Reconnaissance	401,683
2	Initial access	102,090
3	Lateral movement	12,498
4	Exfiltration	25,915
Total sample count = 554,534		

VI. RESULTS AND DISCUSSIONS

This section describes the experimental setup and evaluation methodology, followed by an in-depth analysis of the results.

A. Experimental Setup

All algorithms are implemented in Python 3.13.6 using the Keras framework built on TensorFlow 2.2.0 and evaluated on a MacBook equipped with an Apple M4 chip and 16 GB of RAM. The on-device inference experiments are conducted on a Raspberry Pi 5 using Python 3.11.9 and TMU 0.6.5.

B. Evaluation Methodology

To evaluate classification performance, the models are assessed using precision, recall, and F1-score. Precision reflects the correctness of detected attacks, while recall measures the capability of the IDS to identify actual attacks. The F1-score combines these two metrics into a single measure by balancing precision and recall. In multi-class classification, the F1-score is generally preferred over accuracy, as it accounts for both false positives and false negatives. This is particularly important for imbalanced datasets (e.g., in our case of the MedSec-25 dataset), where accuracy can be dominated by majority classes and may not accurately represent performance across all classes. For instance, failing to detect rare attacks (low recall) or incorrectly classifying benign traffic as malicious attacks (low precision) can significantly impact system reliability. Such trade-offs are not adequately captured by accuracy, whereas the F1-score provides a more comprehensive evaluation. In addition, five-fold cross-validation [25] is utilized to obtain reliable estimates of the evaluation metrics. A confusion matrix is employed to visualize the classification results and analyze class-wise performance. The effectiveness

of the proposed IDS is further validated through comparison with ML classifiers (see Section III-B) as well as state-of-the-art methods from the literature. Moreover, inference time, defined as the duration required by a trained model to produce the prediction for a given input sample during deployment, is measured and compared to assess computational efficiency.

To improve the interpretability of the proposed TM model, class-specific vote scores and clause activation heatmaps are analyzed to explain the classification decisions. A higher vote score for a given class reflects stronger evidence that the input network traffic belongs to that class, thereby indicating a more confident classification decision. In addition, feature-level contributions are examined to identify the key attributes influencing correct predictions. The performance metrics are defined as [28]:

$$\text{Precision} = \frac{TP}{TP + FP}, \quad \text{Recall} = \frac{TP}{TP + FN}, \quad (4)$$

$$\text{F1-score} = \frac{2 \times (\text{Precision} \times \text{Recall})}{\text{Precision} + \text{Recall}}, \quad (5)$$

where TP , TN , FP , and FN correspond to true positive (accurately detected attacks), true negative (correctly classified benign traffic), false positive (benign traffic incorrectly classified as attacks), and false negative (attack instances that remain undetected), respectively.

C. Classification Analysis

1) *Data Pre-processing*: The dataset (see Table II) exhibits class imbalance and contains a small number of missing and duplicate samples. To enhance data quality, preprocessing is performed to eliminate these samples. Despite this cleaning process, the dataset remains imbalanced, as depicted in Fig. 3. The dataset is then partitioned into 80% training and 20% testing subsets. Training models on such imbalanced data can lead to degraded performance and a higher rate of false positives. To mitigate this issue, different strategies are adopted for the TM and ML models. For the TM model, the Synthetic Minority Over-sampling Technique (SMOTE) [25] is applied exclusively to the training set to generate synthetic samples for minority classes, as depicted in Fig. 4. In contrast,

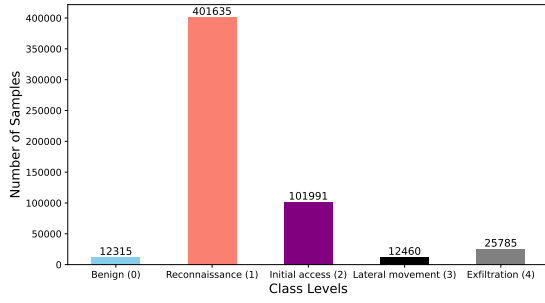


Fig. 3: Class imbalance: Multi-class (five-class) classification.

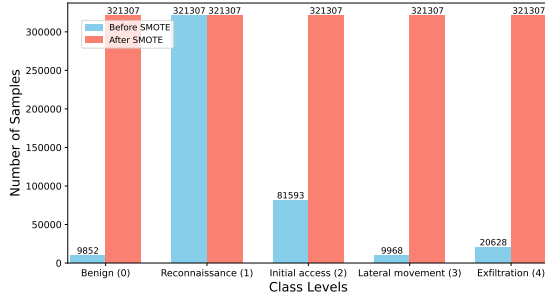


Fig. 4: Balanced training class.

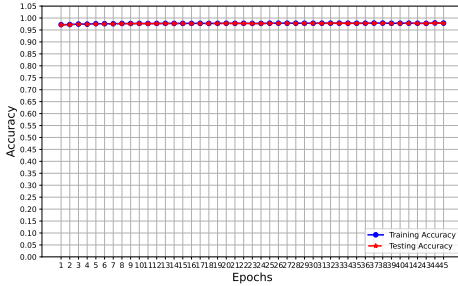


Fig. 5: Training and testing accuracy of the TM model.

for the ML classifiers, class imbalance is handled using the `compute_class_weight` method [25], which assigns higher weights to minority classes and lower weights to majority classes during training. These strategies reduce bias toward majority classes and enhance classification performance.

2) *Classifier Training*: The numerical features are first normalized to a common scale with zero mean and unit variance. This step improves training stability and ensures that all features contribute equally to the learning process. As the TM operates on binary inputs and relies on logical rule formation, these normalized features are further transformed into discrete intervals using the `KBinsDiscretizer` [25], facilitating effective binarization and interpretable clause learning. Similarly, the same preprocessed data (without binarization) is used to train various ML classifiers (see Section III-B). The parameter settings and classification performance of the TM and ML models are summarized in Table III and Table IV, respectively. Additionally, Fig. 5 shows the training and testing accuracy for the TM model, indicating stable learning without overfitting.

Table IV indicates that most classifiers achieve consistently high mean values of precision, recall, and F1-score with minimal variance, except for Naive Bayes and Logistic Regression,

TABLE III: Model parameters.

Model	Parameters
TM	Binarizer: <code>KBinsDiscretizer</code> , <code>n_bins=40</code> , <code>encode=onehot-dense</code> , <code>strategy=quantile</code> , <code>number_of_clauses=2000</code> , <code>T=30</code> , <code>s=15</code> , <code>weighted_clauses=False</code> , <code>Epochs=45</code>
STM	Binarizer: <code>KBinsDiscretizer</code> , <code>n_bins=25</code> , <code>encode=onehot-dense</code> , <code>strategy=quantile</code> , <code>number_of_clauses=1500</code> , <code>T=30</code> , <code>s=20</code> , <code>weighted_clauses=False</code> , <code>literal_sampling=1</code> , <code>max_included_literals=16</code> , <code>absorbing=0</code> , <code>Epochs=50</code>
DT, RF	<code>compute_class_weight</code> method with <code>class_weight=balanced</code>
XGBoost	<code>objective=multi:softprob</code> , <code>eval_metric=mlogloss</code> , <code>tree_method=hist</code> , <code>learning_rate=0.1</code> , <code>max_depth=8</code> , <code>n_estimators=200</code>
LGBM	<code>objective=multiclass</code> , <code>learning_rate=0.1</code> , <code>n_estimators=200</code> , <code>compute_class_weight</code> method with <code>class_weight=balanced</code>
KNN	<code>n_neighbors=5</code>
NB	default settings
LR	<code>solver=lbfgs</code> , <code>max_iter=500</code> , <code>multi_class=multinomial</code> , <code>compute_class_weight</code> method with <code>class_weight=balanced</code>
NN	<code>input layer=79</code> neurons, <code>first hidden layer=64</code> neurons, <code>second hidden layer=32</code> neurons, <code>output layer=1</code> neurons, <code>hidden layer activation function=relu</code> , <code>output layer activation function=softmax</code> , <code>optimizer=adam</code> , <code>loss=sparse_categorical_crossentropy</code> , <code>metrics=accuracy</code> , <code>epochs=10</code> , <code>batch_size=32</code> , <code>verbose=0</code> , <code>compute_class_weight</code> method with <code>class_weight=balanced</code>

TABLE IV: Model performance.

Model	Precision (in %)	Recall (in %)	F1-score (in %)	Inference time (in microseconds μ s)
TM	97.87 ± 0.01	97.83 ± 0.00	97.83 ± 0.00	66.24 ± 1.11
STM	97.38 ± 0.07	97.32 ± 0.08	97.33 ± 0.08	16.89 ± 0.29
DT	94.67 ± 0.20	94.35 ± 0.15	94.51 ± 0.17	0.08 ± 0.04
RF	95.04 ± 0.13	95.21 ± 0.16	95.11 ± 0.04	3.73 ± 0.10
XGBoost	91.75 ± 0.16	97.97 ± 0.06	94.47 ± 0.11	1.77 ± 0.08
LGBM	91.74 ± 0.25	97.95 ± 0.08	94.43 ± 0.19	6.00 ± 0.38
KNN	93.66 ± 0.14	93.10 ± 0.27	93.36 ± 0.15	186.44 ± 3.19
NB	49.91 ± 2.70	56.81 ± 0.31	44.76 ± 2.38	0.65 ± 0.03
LR	58.58 ± 0.12	77.10 ± 0.31	61.19 ± 0.21	0.05 ± 0.00
NN	82.45 ± 0.65	95.19 ± 0.43	87.29 ± 0.74	6.76 ± 0.75

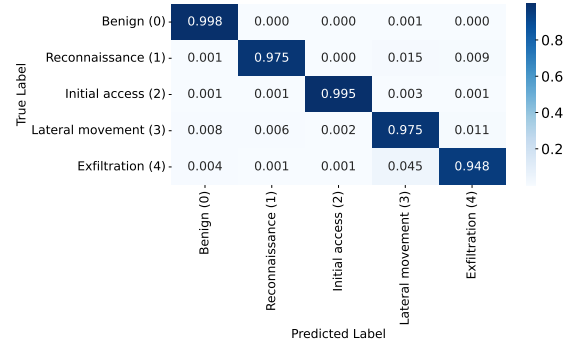


Fig. 6: TM confusion matrix.

which show comparatively lower performance. These results highlight the strong capability of the models to distinguish between benign traffic and various attack classes. Among all models, the TM model achieves the highest F1-score of 97.83%, demonstrating superior classification performance. However, this comes with a slightly higher inference time of 66.24 μ s. In contrast, Logistic Regression offers the fastest inference time of 0.05 μ s, but its F1-score is limited to 61%. The Sparse TM (STM) achieves a reduced inference time

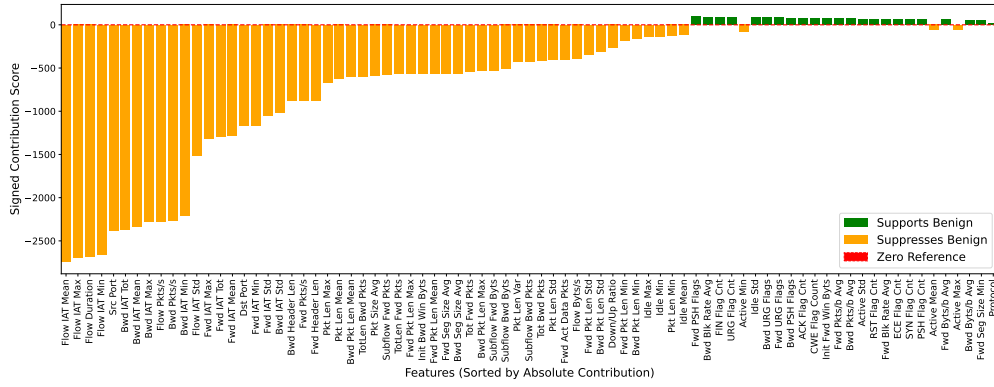


Fig. 7: Feature-level contribution of a Benign sample.

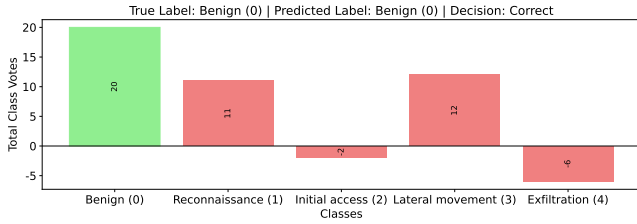


Fig. 8: Class-wise votes of the same Benign sample.

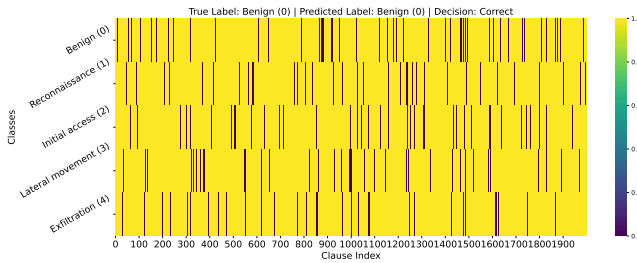


Fig. 9: Clause activation heatmap of the same Benign sample.

(16.89 μ s) compared to the TM model (66.24 μ s), as expected, while maintaining competitive performance.

Next, Fig. 6 presents the confusion matrix of the TM model, highlighting strong diagonal dominance and indicating accurate classification across all five attack classes. The model achieves very high true positive rates for benign and initial access traffic. Similarly, reconnaissance and lateral movement are classified effectively, with only minor confusion between related attacks. The exfiltration class shows some misclassification as lateral movement, likely due to similarities between these attack phases. Overall, the TM model shows robust and reliable detection of various phases of cyberattacks.

3) *TM Interpretability*: To demonstrate the interpretability of the TM model’s decisions, Figs. 7, 8, and 9 illustrate the feature-level contributions, class-wise vote scores, and clause activation heatmap for a benign test sample, respectively. Fig. 7 shows that most features contribute negatively (orange), suppressing non-benign patterns, while a smaller subset provides positive support (green) for the benign class. This indicates that the TM model achieves correct classification by effectively suppressing conflicting patterns. Fig. 8 shows that the benign class attains the highest class vote (20), indicating

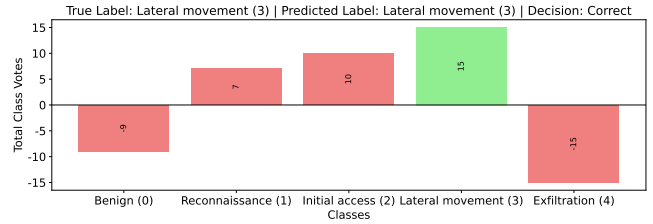


Fig. 10: Class-wise votes of the Lateral movement sample.

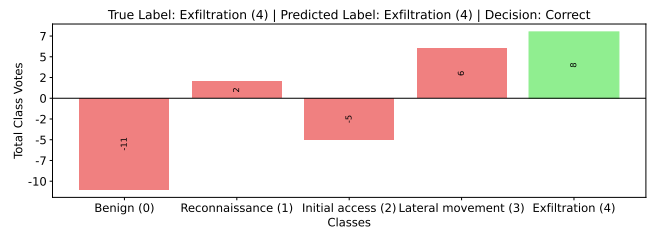


Fig. 11: Class-wise votes of the Exfiltration sample.

normal traffic behaviour. Fig. 9 shows that each cell represents the clause activation status for a given sample, where yellow (1) denotes active clauses and dark purple (0) denotes inactive clauses. The benign class shows a higher number of activated positive clauses, contributing to a larger class vote, while other classes show fewer clause activations. This difference in clause activity results in the highest class vote for the benign class, leading to correct classification. Similarly, Fig. 10 and Fig. 11 illustrate that the lateral movement and exfiltration classes attain the highest votes of 15 and 8, respectively, compared to other classes, indicating malicious network traffic behaviour.

D. On-Device Analysis

Table V shows that the proposed TM and STM provide a balanced trade-off between computational efficiency and resource consumption on the resource-constrained Raspberry Pi. Although TM and STM require higher memory usage than DT, NB, and LR, they maintain moderate CPU usage (around 25%) and smaller model sizes than RF and KNN. In contrast, XGBoost and LGBM achieve fast inference but consume very high CPU resources (around 99%). Moreover, STM achieves slightly better efficiency than TM, making the proposed model suitable for real-time edge-based cyberattack detection.

TABLE V: Edge performance.

Model	Inference time (in μ s)	Memory usage (in KB)	CPU usage (in %)	Model size (in KB)
TM	230.44	161920	25.5	11075.09
STM	222.76	273360	25.9	6028.08
DT	0.26	928	30.8	915.25
RF	17.77	128	25.5	127051.40
XGBoost	8.02	752	98.9	5920.76
LGBM	58.81	480	99.2	3455.24
KNN	3615.08	2256	99.2	277093.31
NB	4.57	1	28.0	7.01
LR	1.05	12208	91.5	4.23
NN	58.40	43856	37.9	110.84

TABLE VI: Comparison with the state-of-the-art methods.

	Model	Precision	Recall	F1-score	Interpretability
Paper [26]	ML Classifier	97.73%	97.83%	97.78%	No
Proposed	Sparse TM	97.38%	97.32%	97.33%	Yes
Proposed	TM	97.87%	97.83%	97.83%	Yes

E. State-of-the-Art Comparison

Table VI demonstrates the superior performance of the proposed TM-based IDS in detecting benign traffic and various phases of attacks on the same dataset. The Sparse TM also achieves comparable performance. Unlike the ML classifier, both TM-based approaches provide interpretability, enabling transparent decision-making through human-readable rules.

VII. CONCLUSIONS AND FUTURE WORK

This work addresses the challenge of detecting different phases of cyberattacks in the IoMT networks by proposing a TM-based IDS model. The model employs an interpretable, rule-driven ML framework that captures attack patterns using propositional logic. The model is trained and evaluated on the MedSec-25 dataset containing realistic cyberattack phases. Experimental results report that the proposed model performs better than ML classifiers and existing state-of-the-art methods, with robustness validated through five-fold cross-validation. Additionally, the model provides explicit decision explanations to enhance transparency. The model is further deployed on an edge device to support real-time on-device inference. The combination of interpretability and high performance makes the proposed model well-suited for IoMT healthcare, where trust, reliability, safety, and timely decision-making are critical. Future work will extend the evaluation to self-developed and multiple public datasets with broader attack variability.

ACKNOWLEDGEMENT

This publication has emanated from the research project SecureIoTM: Ultra-low-energy IoT Intrusion Detection Systems using Logic-based Tsetlin Machines, under Grant Number 342167, funded by the Research Council of Norway.

REFERENCES

- [1] C. Huang, J. Wang, S. Wang, and Y. Zhang, "Internet of Medical Things: A Systematic Review," *Neurocomputing*, vol. 557, p. 126719, 2023.
- [2] Deloitte, "Global Health Care Outlook 2026." [Online]. Available: <https://www.deloitte.com/us/en/insights/industry/health-care/life-sciences-and-health-care-industry-outlooks.html>
- [3] CrowdStrike, "Global Threat Report 2026." [Online]. Available: <https://www.crowdstrike.com/en-us/global-threat-report/>
- [4] L. Diana and D. Paolini, "Overview on Intrusion Detection Systems for Computers Networking Security," *Computers*, vol. 14, p. 87, 2025.
- [5] S. Kundu, S. S. Patkar, S. M. Mishra, and F. Merchant, "A Comprehensive Review of Tsetlin Machines: Concepts, Applications, Analysis, and the Future," *IEEE Internet of Things Journal*, pp. 1–25, 2026.
- [6] O.-C. Granmo, "The Tsetlin Machine—A Game Theoretic Bandit Driven Approach to Optimal Pattern Recognition with Propositional Logic," *arXiv preprint arXiv:1804.01508*, pp. 1–42, 2018.
- [7] B. Nawaal, U. Haider, I. U. Khan, and M. Fayaz, "Signature-based Intrusion Detection System for IoT," in *Cyber Security for Next-generation Computing Technologies*. CRC Press, 2024, pp. 141–158.
- [8] M. Bhavsar, K. Roy, J. Kelly, and O. Olusola, "Anomaly-based Intrusion Detection System for IoT Application," *Discover Internet of Things*, vol. 3, no. 5, pp. 1–23, 2023.
- [9] C. Anitha, C. Komala, C. V. Vivekanand, S. Lalitha, and S. Boopathi, "Artificial Intelligence Driven Security Model for Internet of Medical Things (IoMT)," in *3rd International Conference on Innovative Practices in Technology and Management*. IEEE, 2023, pp. 1–7.
- [10] J. B. Awotunde, K. M. Abiodun, E. A. Adeniyi, S. O. Folorunso, and R. G. Jimoh, "A Deep Learning-based Intrusion Detection Technique for a Secured IoMT System," in *International Conference on Informatics and Intelligent Applications*. Springer, 2021, pp. 50–62.
- [11] N. C. Kavkas and K. Yildiz, "Enhancing IoMT Security with Deep Learning Based Approach for Medical IoT Threat Detection," in *IEEE International Symposium on Digital Forensics & Security*, 2025, pp. 1–5.
- [12] S. Dadkhah, E. C. P. Neto, R. C. Molokwu, and A. A. Ghorbani, "CICIoMT2024: A Benchmark Dataset for Multi-Protocol Security Assessment in IoMT," *Internet of Things*, vol. 28, p. 101351, 2024.
- [13] O. Gunvaldsen, H. B. Thorsen, P.-A. Andersen, O.-C. Granmo, and M. Goodwin, "Towards IoT Anomaly Detection with Tsetlin Machines," in *IEEE International Symposium on the Tsetlin Machine*, 2023, pp. 1–8.
- [14] R. K. Jaiswal, M. Elnourani, S. Deshmukh, and B. Beferull-Lozano, "Leveraging Transfer learning for Radio Map Estimation via Mixture of Experts," *IEEE TCCN*, vol. 12, pp. 846–863, 2025.
- [15] R. Jaiswal, M. Elnourani, S. Deshmukh, and B. Beferull-Lozano, "Location-free Indoor Radio Map Estimation using Transfer learning," in *97th Vehicular Technology Conference*. IEEE, 2023, pp. 1–7.
- [16] E. Ahishakiye, L. Nkalubo, F. Kanobe, D. Taremwa, B. A. Nantongo, and S. Ahimbisibwe, "Enhanced Cervical Cancer Classification using Convolutional Tsetlin Machines with Transfer Learning," *Discover Artificial Intelligence*, vol. 6, no. 1, p. 301, 2026.
- [17] R. Jaiswal, P.-A. Andersen, L. R. Cenkermaddi, L. Jiao, and O.-C. Granmo, "A Tsetlin Machine-driven Intrusion Detection System for Next-Generation IoMT Security," in *7th Silicon Valley Cybersecurity Conference*. IEEE, 2026, pp. 1–8.
- [18] L. Breiman, J. Friedman, R. A. Olshen, and C. J. Stone, *Classification and Regression Trees*. Chapman and Hall/CRC, 2017.
- [19] R. K. Jaiswal and R. Dubey, "CAQoE: A Novel No-reference Context-aware Speech Quality Prediction Metric," *ACM Trans. on Multimedia Computing, Comms. and Applications*, vol. 19, no. 1s, pp. 1–23, 2023.
- [20] E. Jedari, Z. Wu, and M. Saif, "Wi-Fi based Indoor Location Positioning Employing Random Forest Classifier," in *IEEE International Conference on Indoor Positioning and Indoor Navigation*, 2015, pp. 1–5.
- [21] T. Chen and C. Guestrin, "Xgboost: A Scalable Tree Boosting System," in *22nd ACM SIGKDD International Conference on Knowledge Discovery and Data Mining*, 2016, pp. 785–794.
- [22] G. Ke, Q. Meng, and T. Finley, "Lightgbm: A Highly Efficient Gradient Boosting Decision Tree," in *31st Conference on Neural Information Processing Systems*, 2017, pp. 1–9.
- [23] E. Alpaydin, *Introduction to Machine Learning*. MIT press, 2020.
- [24] S. E. Mathe, H. K. Kondaveeti, S. Vappangi, S. D. Vanambathina, and N. K. Kumaravelu, "A Comprehensive Review on Applications of Raspberry Pi," *Computer Science Review*, vol. 52, p. 100636, 2024.
- [25] R. Bhagwat, M. Abdolahnejad, and M. Moocarme, *Applied Deep Learning with Keras: Solve Complex Real-life Problems with the Simplicity of Keras*. Packt Publishing Ltd, 2019.
- [26] W. Almobaideen, M. Abdullah, U. Alam, S. B. Hussain, and A. Bouharat, "MedSec-25: Creating an IoMT Dataset for a Healthcare IoT Environment," in *7th International Conference on Blockchain Computing and Applications*. IEEE, 2025, pp. 628–634.
- [27] MITRE, "Mitre Att&ck Framework 2026," <https://attack.mitre.org/>.
- [28] R. Jaiswal, "Performance Analysis of Voice Activity Detector in Presence of Non-stationary Noise," in *11th Int. Conf. on Robotics, Vision, Signal Processing and Power Applications*. Springer, 2022, pp. 59–65.